Journal of Materials Science: Materials in Electronics (2019) 30:9742–9750
https://doi.org/10.1007/s10854-019-01309-w

# Polymer–chalcogenide glass nanocomposites for amplitude–phase modulated optical relief recording

J. Burunkova[1] · S. Molnar[2] · V. Sitnikova[1] · D. Shaimadiyeva[1] · G. Alkhalil[1] · R. Bohdan[2] · J. Bako[3] · F. Kolotaev[1] · A. Bonyar[4] · S. Kokenyesi[2]

Received: 21 February 2019 / Accepted: 8 April 2019 / Published online: 12 April 2019


**Abstract**
The main objective of this work was to combine the positive characteristics of transparent photopolymers and light-sensitive chalcogenide glasses, with aim to improve the amplitude–phase modulation characteristics of in situ optically recorded photonic elements on the surface, and in the bulk of thick composite layer on a given substrate. The positive results were obtained due to the developed technology routes of nanocomposite (NC) fabrication by intermixing selected, optically tunable, VIS–NIR transparent and high refractive index As-S (Se) nanoparticles (NPs) produced by chemical dissolution, and acrylate monomers with initiators. Subsequent photopolymerization of such nanocomposite occurs during optical recording photonic elements and is supplemented by mass-transport processes, which enhance relief parameters. Structure, optical parameters of the new light-sensitive media and conditions of one step recording of optical elements in it were investigated.

## 1 Introduction

Composite materials are usually developed to combine positive or unique characteristics of selected components in a new material. Nowadays nanocomposites play an essential role in the development of smart, poly-functional materials [1, 2]. For example, combining polymer and quartz glass nanoparticles results new, flexible glassomer-type material [3]. Polymer nanocomposites containing organic and inorganic components were developed and applied for optical, holographic recording of different photonic elements like gratings, two- or even three dimensional structures [4–8]. The limiting factors for optical application of these materials may be connected with high scattering levels, which essentially decrease at comparatively low concentrations and sub-wavelength, nanometer-scale dimensions of NPs [9].

In our previous papers [7, 8, 10, 11] we described acrylate nanocomposites containing $SiO_2$, ZnO, Au nanoparticles for optical recording of diffraction gratings in thick layers, where the inhomogeneous redistribution of nanoparticles due to the non-uniform optical field stimulated polymerization, accompanied with nanoparticles diffusion, increases the light-modulation characteristics. Since the differences in the refractive indices of components, as well as of the recorded relief are not essential (the refractive index $n$ of $SiO_2$ is near 1.5 in the visible spectral region and the index of most polymers is 1.4–1.5) the modulation is still rather small. But at the same time $n$ matching in such material system and small, nm-sizes of particles support the high transparency of the nanocomposite.

Chalcogenide glasses (ChG) from As (Ge)-S (Se,Te) and similar systems possess unique broad transparency spectra up to 10–20 μm, high refractive index ($n > 2$), high optical nonlinear characteristics and their optical parameters can be reversibly treated by illumination-annealing [12, 13]. Since chalcogenide glasses present a unique class of materials, much like the organic polymers, they are called sometimes inorganic polymers and so their compatibility in a nanocomposite can be ensured.

Inserting high refractive index chalcogenide glass nanoparticles to the photopolymer may increase the modulation characteristics, as well as produce materials with high transparency, optical nonlinearity in the infrared spectral region.

✉ S. Molnar
molnar.ms.sandor@science.unideb.hu

[1] ITMO University, St. Petersburg, Russia

[2] Institute of Physics, University of Debrecen, Debrecen, Hungary

[3] Faculty of Dentistry, University of Debrecen, Debrecen, Hungary

[4] Department of Electronics Technology, Budapest University of Technology and Economics, Budapest, Hungary

The *nm* sizes of particles at comparatively low concentrations in a polymer matrix ensure small scattering levels in VIS–IR spectral regions.

In this work we used nanoparticles of $As_2S_3$, As-Se chalcogenide glasses (refractive index in the VIS–NIR region is near 2.2) to create light-sensitive nanocomposites with additional functionalities in comparison with previously developed ones [7, 8]. Additional advantage of such material is the possibility to change the optical parameters of the inserted semiconductor chalcogenide glass particles (optical absorption edge and refractive index) by special illumination and annealing. This creates the possibility to stimulate the parameters of the final optical element. The fabrication route of such nanocomposites, structural investigations and measurements of optical recording parameters are presented.

## 2 Experimental

### 2.1 Materials used

Chalcogenide glasses $As_2S_3$ and $As_{20}Se_{80}$, obtained by direct synthesis of high-purity elements in quartz ampules were used as components for nanocomposite fabrication. The dissolution of chalcogenide glasses were investigated in diethylamine (DEA), propylamine (PrA), monoethanolamine (MEA) and triethanolamine (TEA), but the best results were obtained using diethylamine so its application will be shown below.

Among the number of possible monomers as matrix, the next materials were selected and used: diurethane dimethacrylate, mixture of isomers (UDMA, ≥ 97%, Aldrich № 436909), isodecyl acrylate (IDA, Aldrich № 408956), 2-phenoxyethyl acrylate (PEA, Aldrich № 408336-250ML), 2-(dimethylamino) ethyl acrylate (AmAc, Aldrich № 330957).

The selected initiator for polymerization—bis(cyclopentadienyl)bis[2,6-difluoro-3-(1-pyrryl)phenyl] titanium (Irq784, CAS № 125051-32-3) is sensitive up to 550 nm, it may be used for photo-polymerization by green laser.

### 2.2 Measurement technics

Optical transmission spectra of polymer, chalcogenide and nanocomposite layers on glass substrates were measured in visible-near infrared spectral region by standard method with Shimadzu UV3600 spectrophotometer. Optical transmission spectra of liquid monomers and nanocomposites were measured in thick layers, limited in size and thickness by spacers between glass substrate and polyester cover. ATR spectral measurements were made with Bruker Tensor-37 ATR-Miracle-Pike equipment. Structural investigations of nanocomposites were made on a Hitachi S-4300 SEM, JEM-2000FXII TEM and an XRD equipment. Optical recording of diffraction gratings was done by $\lambda = 532$ nm or $\lambda = 633$ nm emitting lasers. AFM measurements of optically recorded surface reliefs were performed with Veeco diInnova atomic force microscope in tapping regime.

### 2.3 Sample preparation

The fabrication method, preparation of polymer–chalcogenide nanocomposite with new functional parameters was one of the principal tasks of our work. The first step of this route is to fabricate chalcogenide glass nanoparticles (ChG NPs). For NP fabrication we tested the applicability of a laser ablation method to obtain $As_2S_3$ nanoparticles directly in the proper monomer matrix by ablation of the bulk glass sample surface with pulsed Nd:YAG laser ($\lambda = 532$ nm, power 8 mJ, power density 4 J/cm$^2$, 10 Hz repetition rate). The process yield was low, the concentration of 15–50 nm glass nanoparticles in stable transparent colloid was small, less than 1 wt%. Increasing the concentration of NPs at the vicinity of the ablated surface results agglomeration, sediment formation in a high-viscosity surroundings, thus this simple, direct physical technology method needs to be further developed. Therefore, we concentrated on the chemical route of producing ChG NPs and composites with the given monomer matrix, which can be used for further investigations of functional photopolymerizable nanocomposite films in mass-production quantities.

Understanding the mechanism of obtaining ChG NPs by chemical route supposes availability of data about successfully intermixing them in the given monomers without aggregation and further stability of the mixture up to the polymerization, i.e. light-induced creation of given optical and structural relief.

We started with known and widely investigated light-sensitive $As_2S_3$ and $As_{20}Se_{80}$ compositions. As it is known, $As_2S_3$ is unstable in alkalines, dissociates roughly. The chemical stability and solubility of ChGs in different solvents like *n*-propylamine and *n*-butylamine is "softer" as was investigated in [14]. According to their data, the chain-layered structure of the glass is broken to amorphous fragments of $As_2S_3$, mostly at chalcogen bonds. NP dimensions were roughly 2–10 nm large. Thus, the $As_2S_3$ dissolved in alkylamides may be considered as a colloidal solution or nanocomposite, consisting of flat clusters with elements of initial glass network, which are limited by broken Sulphur bonds and alkylammonium molecules. These nanoclusters agglomerate in the composite film and can form bigger clusters under certain conditions [15, 16].

The next step of ChG NP creation consists of blending monomers with dissolved chalcogenides. The surface of ChG NPs in amine solutions may be stabilized due to the

introduction of monomers, which possess necessary functional groups like –N–H or –O–H. Evaporation of the solvent results uniform stable nanocomposite, since the monomers not only form a plastic polymer matrix but also modify the surface of ChG NPs, preventing to a certain degree their aggregation. So, the selection of monomers was done considering the presence of functional groups, which may stabilize ChG NPs. UDMA was selected due to the presence of N–H groups, monomer PEA—the presence of phenyl ring and monomer AmAc—the presence of $–N–(CH_3)_2$ group. As a result of experimental selections, a nanocomposite suitable for in situ optical relief recording was developed. This composition consists of chalcogenide glass (7.5 wt% of monomer mixture), crushed to micro-nanometer size particles and solved in diethylamine. Then the monomer mixture was added to this solution by stirring the composite for 24 h and Irgacure 784 initiator in chloromethylene was added (4 wt% of monomer mixture). The solvent was evaporated in Nitrogen atmosphere and the remaining composite was continuously weighted until constant values. Optically transparent, stable nanocomposites were obtained this way, their compositions are presented in Table 1.

To produce solid ChG nanocomposite films for optical measurements, a certain amount of monomer solution, presented in Table 1, was placed on a glass substrate, limited by a 30 µm spacer and covered by polyester film. Further it was polymerized by UV radiation (10 mW/cm$^2$, Osram lamp) for 30 min. The resulting solid films were homogeneous, transparent and bright yellow colored.

Optical holographic recording was used on the samples of Table 1, but instead of a uniform photopolymerization, as written above, the laser interference or other pattern was projected on the sample. The standard two-beam interference scheme was used, with a LCS-DTL-317 laser, emitting at 532 nm, power density 2 mW/cm$^{2,}$ the recording time was 30 min, like used in [8]. The diffraction efficiency (DE) was measured by additional 635 nm laser beam at Bragg angle as the ratio of the diffracted and incident beam intensities. He–Ne laser emitting at $\lambda = 633$ nm (grating period $\Lambda = 15$ µm with power densities 6 mW/cm$^2$) was also used for recording on As-Se containing nanocomposites. The exposition time was 30 min.

**Table 1** Nanocomposites obtained by chemical route

| № | Monomer ratios (wt%) | | | Initiator Irq784 (wt%) | ChG (wt%) |
|---|---|---|---|---|---|
| 11h | UDMA 80 | IDA 10 | PEA 10 | 4% | 7.5% $As_2S_3$ |
| 14h | UDMA 70 | AmAc 20 | PEA 10 | | 7.5% $As_2S_3$ |
| 20h | UDMA 70 | AmAc 20 | PEA 10 | | 7.5% $As_{20}Se_{80}$ |

Separate samples of thin (~2 µm) films of chalcogenide glass on silica glass substrates were prepared by thermal evaporation in vacuum. These were used for optical spectral measurements and for comparison with optical spectra of nanocomposite films.

## 3 Results and discussion

Optical transmission spectra of the typical monomer composite, nanocomposite and of the vacuum-evaporated $As_{20}Se_{80}$ chalcogenide thin film are presented in Fig. 1.

Since the concentration of ChG NPs is small, 2.6 vol% or 7.5 wt%, in the polymer NC film, which originally in pure state is transparent in all visible spectral region, the absorption edge of NC is shifted towards UV due to the contribution of two added components.

The small dimensions of ChG NPs, as determined from TEM measurements (see Fig. 2), at low concentrations, may add further blue shift of spectra due to the quantum confinement effects without noticeable scattering. Some changes of NP distribution may occur during the sample preparation for TEM investigations.

The XRD measurements show that the polymer–ChG NC is amorphous, as much both components are initially amorphous.

As it was mentioned above, stable monomer—ChG nanocomposites may be produced due to the capping of ChG NPs by monomers. Such process was supported by measurements of FTIR-ATR spectra in pure monomers and

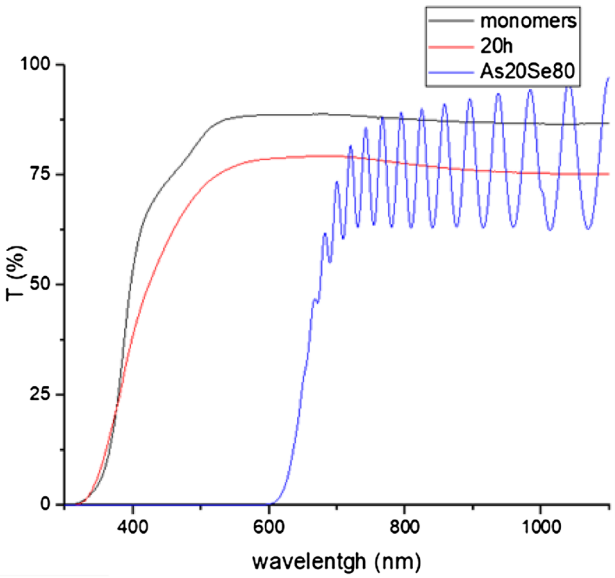


**Fig. 1** Optical transmission spectra of 20h composite and monomer (without ChG) layer with thickness 15 µm, and pure $As_{20}Se_{80}$ film (2 µm), evaporated in vacuum onto glass substrate

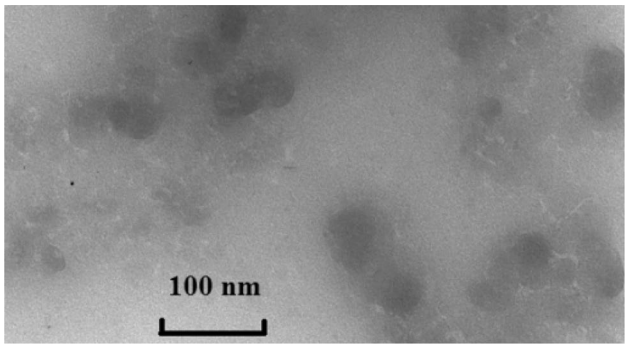


**Fig. 2** TEM picture of the nanocomposite

nanocomposites. Series of FTIR-ATR spectra measured in different IR spectral ranges are presented separately in Fig. 3a–d for better resolution and analysis (sample 14h). Similar data were obtained for other nanocomposites from Table 1.

FTIR-ATR spectra of the samples, obtained from a mixture of monomers in composite 14 (Table 1) without ChG NPs correspond with literature data [17–22] for urethane polymers and polymers with phenyl fragment. Characteristic wide band at 3350 $cm^{-1}$ corresponds to the stretching vibrations of NH-groups (Amide A) and other bands at 1710 $cm^{-1}$ (Amide I), 1540 $cm^{-1}$ (Amide II), 1300–1250 $cm^{-1}$ (Amide III) as well as 1220 $cm^{-1}$ ($\nu$(C–O)) and strong band at 1150 $cm^{-1}$ ($\nu_{asym}$(O–C–O)). Characteristic absorption bands of phenyl fragment of PEA are visible in the 1420–1600 $cm^{-1}$ range. Besides these, there are bands in the 1000–650 $cm^{-1}$ spectral range, which correspond to the out of plane deformational vibrations of C–H bonds of benzene circle, but in this range are also located the in-plane rocking vibrations of –N–H group.

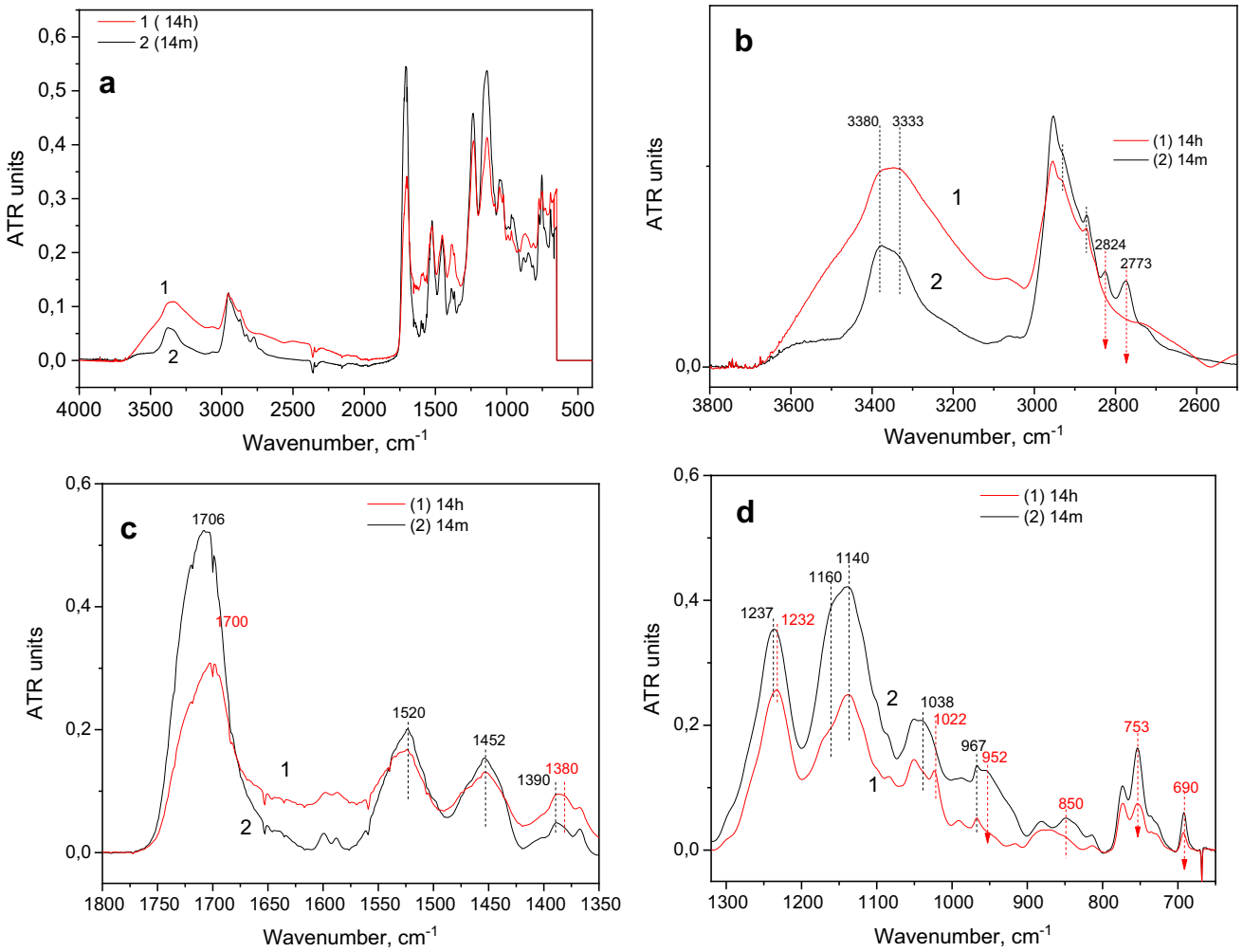


**Fig. 3** FTIR-ATR spectra for the 14h nanocomposite (curve 1) and pure monomer matrix (composition 14 m) without ChG nanoparticles (curve 2) measured in different spectral ranges (**a**–**d**). **a** General, **b**–**d** selected ranges

Adding $As_2S_3$ nanoparticles to the mixture of monomers (nanocomposite 14h in Table 1) causes the next changes in FTIR-ATR spectra:

- intensity of the 753 $cm^{-1}$ band essentially decreases (γCH of the benzene ring and vibrations of –N–H group) as well as the 690 $cm^{-1}$ band (γCC of the benzene ring). These support the stabilization of NPs by the presence of associated bonds of benzene ring and –N–H group,
- intensities of 950 $cm^{-1}$, 1038 $cm^{-1}$ and 1160 $cm^{-1}$ bands decrease, that shows the decrease of intensities of stretching vibrations in $\nu_{sym}C_{ph}$–C–O and νC–N, $\nu_{asym}$C–O–C(=O),
- the ratio of 1237/1140 $cm^{-1}$ band intensities changes, that supports the role of $\nu_{asym}$C–O–C(=O) bond in the stabilization of NPs. The absorption band intensity at 850 $cm^{-1}$ (νC–C–O–C(=O)–C($H_3$)) decreases, that also supports the stabilization of NPs by oxygen.

These and further changes in FTIR vibrational spectra of nanocomposites, connected with changes in benzene ring vibrations, in bands of groups containing oxygen and nitrogen (C–O, N–H and others) testify that donor–acceptor bonds are formed between these groups and $As_2S_3$ NP surfaces. Such a capping effect restricts further aggregation of NPs in the monomer matrix after the evaporation of the solvent (which initially, before evaporation restricts aggregation in solution) and increases the affinity of inorganic NPs in organic media, supporting their uniform distribution during intermixing and movement in the mass-transport processes during optical recording as well.

### 3.1 Stimulated changes of optical parameters in NC films

New functionality and applications of the developed nanocomposites for optical recording or in certain photonic elements highly depends on the properties of given ChG NPs, which can be varied in pure, high refractive index ChG films by additional illumination and annealing [12, 13].

Nanocomposite 14h was selected for such investigations, since green laser light can be used as for polymerization as for as additional treatment of ChG NPs optical parameters.

First, the calculation of refractive index of 14h nanocomposite was realized. Earlier we tested some models (proposed by Garnet Maxwell [23], Wiener [24, 25], Bruggeman [26], Lichtenecker [27]) of the calculation of relative permittivity of composite materials. We used these methods for analyzing the experimental data of [28] for refractive index determination of hybrid films $As_{42}S_{58}$ in PMA (very similar to our sample) at $n_{polymer} = 1.45$ and $n_{As42S58} = 2.32$ (at 633 nm) in wide range of $As_{42}S_{58}$ nanoparticle concentrations. These tests showed that all these models give good enough correlation with experimental data for such nanocomposite. Better correlation was observed in the case of the model proposed by Garnet Maxwell [23, 29], where the calculation of relative permittivity of composite materials was realized at low concentration of the included materials in a matrix.

Without absorption the refractive index ($n$) of nonmagnetic materials:

$$n(\omega) = \sqrt{\varepsilon(\omega)} \tag{1}$$

where $\omega$—frequency of the light wave, $n(\omega)$—refractive index. Based on the model of relative permittivity of composite materials of Garnet Maxwell [23], the refractive index of the nanocomposite can by presented as:

$$n_{eff} = n_{polymer} \cdot \sqrt{\frac{1 + 2 \cdot f_{ChG} \cdot \left[\left(n_{ChG}^2 - n_{polymer}^2\right) \Big/ \left(n_{ChG}^2 + 2 \cdot n_{polymer}^2\right)\right]}{1 - f_{ChG} \cdot \left[\left(n_{ChG}^2 - n_{polymer}^2\right) \Big/ \left(n_{ChG}^2 + 2 \cdot n_{polymer}^2\right)\right]}} \tag{2}$$

where $n_{polymer}$—refractive index of polymer matrix, $n_{ChG}$—refractive index of ChG, $n_{eff}$—refractive index of nanocomposite, $f_{polymer}$—volume content of polymer, $f_{ChG}$—volume content of ChG nanoparticles.

Although the very simple approximation also gives good enough correlation with the experiment:

$$n_{eff} = n_{polymer} \cdot f_{polymer} + n_{ChG} \cdot f_{ChG} \tag{3}$$

We calculated the dependence of the refractive index of 14h nanocomposite on volume content of $As_2S_3$ nanoparticles using formulae 2 and 3. These dependences (at 635 nm) are presented in Fig. 4 .

In the case of 14h nanocomposite from Table 1 we have ≈ 2.6% volume content of ChG NPs. The curve 1 from

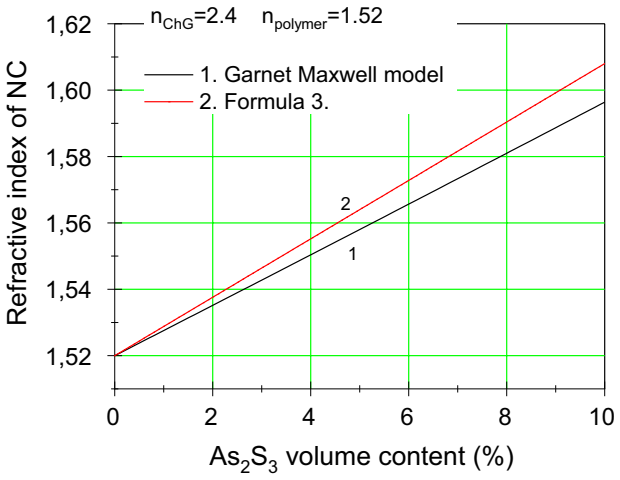


**Fig. 4** Dependence of the refractive index of 14h nanocomposite on volume content of $As_2S_3$ nanoparticles (1—Garnet Maxwell model, 2—Formula 3)

Fig. 4 shows that the refractive index of the composite at 2.6% volume content of ChG NPs is close to 1.54.

Varying between the refractive index of the bulk glass (2.4) and our polymer (1.49) as a weighted average based on the volume fractions of each in the film at non absorbing wavelengths, we got that for 14 h the refractive index is approximately 1.52. It is in accordance with data in [28]. So it is possible to produce uniform polymer–ChG NC with higher average refractive index, which may be further modulated during recording surface/volume optical structures or even afterwards, in a recorded element, due to the variability, light and thermal sensitivity of chalcogenide glass parameters. Further we investigated these possibilities.

We measured optical transmission spectra of the pure, initial components of 14h nanocomposite (monomers and $As_2S_3$ ChG layers) and 14h nanocomposite layer before and after heat treatment and illumination (Fig. 5). The transmission spectra were used for calculation of $(\alpha h\nu)^m$ vs $h\nu$ dependences (Fig. 6), because these dependences are more informative. The calculations of the band gap (Table 2) of components (monomer, $As_2S_3$) and 14h nanocomposite before and after the heat treatment and illumination were based on standard method for analysis of curves $(\alpha h\nu)^m$ vs $h\nu$. In $(\alpha h\nu)^m$, m depends on the type of bandgap of the material: m = 2 for direct bandgap material, m = 1/2 for indirect bandgap material. For chalcogenide glass the model of Urbach tail and indirect band gap is applicable [30, 31]. All functions $(\alpha h\nu)^m$ were normalized to be presentable on one graph.

From Fig. 6 one can see, that the bandgap for an $As_2S_3$ layer (2.27–2.35 eV) is close to the bandgap of 14h nanocomposite (2.08–2.25 eV). The bandgap of the ChG NC is slightly lower than the bandgap of the $As_2S_3$ layer. It could be connected to the state of $As_2S_3$ particles in nanocomposite, i.e. structure, deformations, charging.

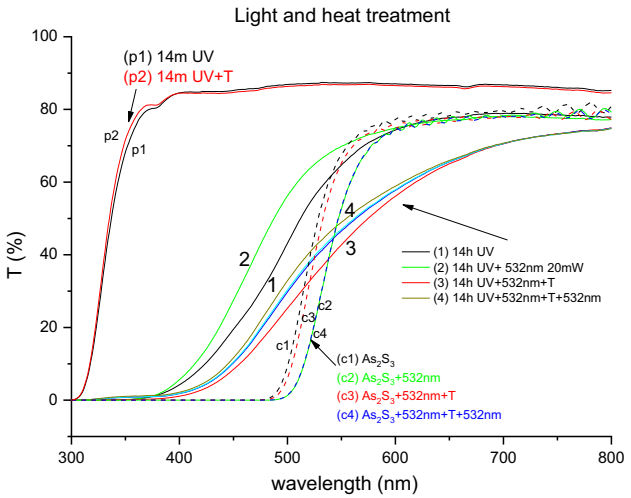


**Fig. 5** Transmission spectra for pure monomer 14 m (curve p1–p2), $As_2S_3$ layer (curve c1–c4) and $As_2S_3$ ChG nanocomposite 14h (curve 1–4). Before and after heat treatment and illumination (T-heat treatment, UV and 532 nm-illumination)

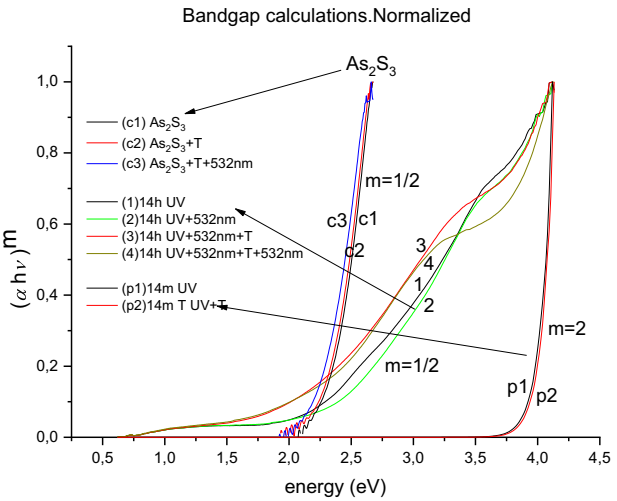


**Fig. 6** Normalized $(\alpha h\nu)^m$ vs $h\nu$ dependences on heat treatment and illumination for components (monomer 14 m (curve p1–p2), $As_2S_3$ (curve c1–c4)) and $As_2S_3$ ChG nanocomposite 14h (curve 1–4) dependence. Here: m = 2 for direct bandgap, m = 1/2 for indirect bandgap materials (T-heat treatment, UV and 532 nm-illumination)

Comparing these results, one can see that the nanocomposite behaves differently than the chalcogenide materials in a base equilibrium state, since pure $As_2S_3$ layer undergoes photodarkening upon illumination (Fig. 5, 6, Table 2). The pure polymer matrix does not change after additional, post-polymerization illumination. The pure polymer matrix is slightly bleached (increasing of polymer matrix bandgap from 3.96 to 3.98 eV Table 2) by heat treatment. It can be connected with the reordering of the structure. The annealing of the polymer in a first cycle also may evaporate the minimal remaining solvents from the polymer as well as volume contraction may occur.

Heat treatment also removes some of the light induced (532 nm irradiation) photodarkening in pure $As_2S_3$ layer (Figs. 5, 6) and the band gap increases from 2.27 to 2.33 eV (Table 2). But if the $As_2S_3$ layer was in a metastable initial state, after heat treatment it returns to a more stable state, which still may be little different from the as-deposited state. The next additional band-gap illumination on $As_2S_3$ turns it back to its photodarkened state with a bandgap equal to 2.27 eV (Table 2).

There is no noticeable transmission change in the longer wavelength region (Figs. 5, 6). These data agree with small concentration of added ChG NPs and so with the comparatively small addition to the refractive index change in the nanocomposite. At the same time light-stimulated bleaching of pure ChG layers usually testify the non-equilibrium state of the glass structure [12, 13]. After heat treatment of the

**Table 2** Explaining processes for Figs. 5 and 6

| № | Material | Influence (T—heat treatment, UV and 532 nm—illumination) | Band gap (eV) | Process(es) |
|---|---|---|---|---|
| p1 | 14 m | UV | 3.96 | Polymerization, contraction of monomer (polymer) |
| p2 | 14 m | UV + T (150 °C, 1 h) | 3.98 | Bleaching determined by contraction of polymer |
| c1 | $As_2S_3$ | As deposited | 2.35 | |
| c2 | $As_2S_3$ | As deposited + 532 nm (85 mW, 100 min) | 2.27 | Darkening determined by photo-structural transformations: defect generation |
| c3 | $As_2S_3$ | As deposited + 532 nm (85 mW, 100 min) + T (150 °C, 1 h) | 2.33 | Bleaching due to the annealing, defect relaxation |
| c4 | $As_2S_3$ | As deposited + 532 nm (85 mW, 100 min) + T (150 °C, 1 h) + 532 nm (85 mW, 5 min) | 2.27 | Darkening determined by illumination, defect generation |
| 1 | 14h | UV | 2.2 | Polymerization and contraction of polymer. Stress generation in $As_2S_3$ is possible |
| 2 | 14h | UV + 532 nm (30 min, 20 mW) | 2.25 | Photo-induced softening of ChG NP, decreasing stress in nanoparticles is possible |
| 3 | 14h | UV + 532 nm (30 min, 20 mW) + T (150 °C, 1.5 h) | 2.08 | Heating and cooling process generates two processes in polymer: expansion and contraction |
| 4 | 14h | UV + 532 nm (30 min, 20 mW) + T (150 °C, 1.5 h) + 532 nm (30 min, 20 mW) | 2.08 | The light cannot decrease the stress in the contracted polymer |

nanocomposite, for an hour or more, at T = 423 K (which is close to the softening temperature Tg of $As_2S_3$ but not high enough to damage the polymer matrix) we noticed darkening of the sample (Figs. 5, 6) and decreasing the bandgap from 2.25 to 2.08 eV, that is the result of $As_2S_3$ nanoparticles darkening similar to $As_2S_3$ layer darkening (Table 2).

Depending on the dose, additional illumination can cause bleaching even after heat treatment, but the sample cannot reach the initial state like in a fresh polymerized sample (Figs. 5, 6). All these stimulated changes show the possibility to influence the optical parameters of the polymer–chalcogenide nanocomposite by optical irradiation and/or heat treatment. The details of the mechanism may include the known reversible changes of transmission and refractive index of chalcogenide glasses within amorphous phase [12, 13], as well as some light- and heat-stimulated changes in polymer matrix structure, appearance of stresses, change of viscosity, which influence ChG nanoparticles, and so on. Important is that this way we can realize fine tuning of certain optical elements like gratings, photonic crystals, waveguides during their one-step recording or in the fabricated element, especially at higher concentrations of chalcogenide glass nanoparticles.

## 3.2 Application for holographic grating recording

Besides formation of a thick volume hologram (Table 3), the AFM measurements showed also the presence of surface depth modulation, as it is usual in the polymer-NC [4, 5, 7–9]. Data for long-period grating recorded in NC 14h are presented in Fig. 7.

**Table 3** Diffraction efficiency of volume gratings, recorded in developed nanocomposites

| Polymer–ChG nanocomposite | Diffraction efficiency (%) |
|---|---|
| 11h | 6 |
| 14h | 20 |
| 20h | 47 |

AFM investigations showed sinusoidal relief with rather smooth surface at 15 μm period, as well as for smaller ones (2 μm). The depth profiles at the given recording conditions show 520–530 nm modulation. We compared the input of surface modulation and ChG NP redistribution to the diffraction efficiency (DE) and found, that 20% DE in transmission mode is mostly connected with pure Δn redistribution between valleys and peaks of the thick volume hologram. It follows from the next considerations.

The influence of green light (532 nm) on changes of reflection from the surface of 14h nanocomposite was measured. This measurement shows that illumination increases the refraction index of 14h nanocomposite with $\Delta n_{532\ nm} = 0.006$. It is expected that relative and absolute changes of refractive index at 633 nm and 532 nm are close. The data of diffraction efficiency of 14h nanocomposite (Table 3) shows that this Bragg grating has a diffraction efficiency equal to 20%. Kogelnik's formula gives the modulation of refractive index (Δn):

$$\Delta n = \frac{\lambda \cos\theta_B \arcsin\sqrt{\eta}}{\pi d} \quad (4)$$

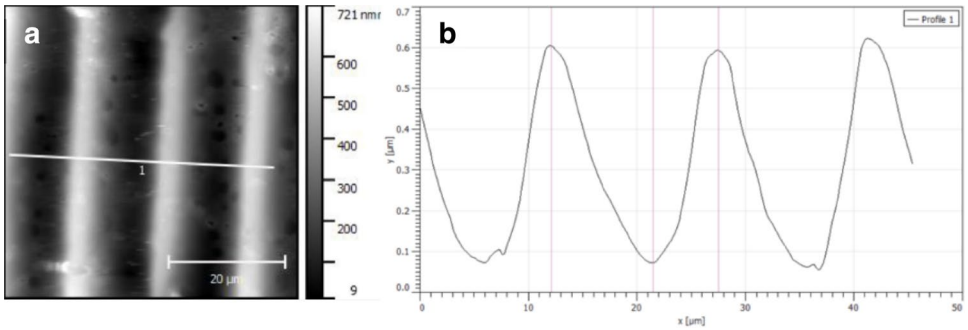


**Fig. 7** AFM picture of the grating recorded in 14h nanocomposite (**a**) and its surface profile (**b**)

where $\theta_B$—the Bragg angle for the recorded grating (9.1° at $\lambda = 635$ nm), d—the grating period (2 µm), η—DE. From this formula it is possible to calculate the maximum deviation of the refractive index $\Delta n = 0.046$. It is larger than the refractive index change by green light illumination ($\Delta n_{532nm} \approx \Delta n_{635nm} = 0.006$). This efficient Bragg diffraction in a volume hologram can be explained by diffusion of ChG nanoparticles and monomers in nanocomposite medium during the recording and local, periodical change of the refractive index of the nanocomposite. It was shown (Fig. 4.) that the average refraction index of 14h nanocomposite ($n_{nc}$) at 2.6% volume content (7.5% w% from Table 1) of ChG nanoparticles is close to 1.54 and the refractive index of pure polymer is $n_{polymer} = 1.52$.

The refractive index distribution has close to linear dependence on concentration of nanoparticles (Fig. 4). If the minimum refractive index is equal to the refractive index of the pure polymer (1.52), then the maximum refractive index of the recorded grating is 1.56 and the deviation of it is 0.04. Therefore, the periodical mass distribution of ChG NPs and of the refraction index ($\Delta n = 0.006$) of $As_2S_3$ nanoparticles in periodical structure explains this high (0.046) amplitude of refraction index modulation.

## 4 Conclusion

The chemical fabrication route of acrylate monomer–chalcogenide nanocomposites was developed. Structural investigations and measurements of optical recording parameters were performed and it was established, that the monomer compositions are uniform, transparent with increased average refractive index even at comparatively low (~ 3% volume) concentration of ChG NPs. These nanoparticles are intermixed to the selected monomer blend without aggregation due to the capping effects of NPs by monomers.

The complex relief formation with redistribution of chalcogenide nanoparticles in the interference light field was realized. The direct recording of amplitude- and phase-modulated volume holograms with high efficiency (up to 47%) was made by green laser light and connected with mass-transport in monomers, diffusional redistribution of nanoparticles. The light- and heat-stimulated bleaching-darkening of nanocomposite layers show the possibility to influence the parameters of recorded optical elements.

**Acknowledgements** Open access funding provided by University of Debrecen (DE). Authors acknowledge the financial support of the GINOP-2.3.2-15-2016-00041 project. The technical support of Dr. L. Daroczi in microscope measurements is highly acknowledged.



## References

1. D.R. Paul, L.M. Robeson, Polymer **49**(15), 3187–3204 (2008)
2. J.P.Y. Kao, K. Thorkelsson, P. Bai, B.J. Rancatore, T. Xu, Chem. Soc. Rev. **42**(7), 2654–2678 (2013)
3. F. Kotz, N. Schneider, A. Striegel, A. Wolfschläger, N. Keller, M. Worgull, W. Bauer, D. Schild, M. Milich, C. Greiner, D. Helmer, B.E. Rapp, Adv. Mater. **30**, 29 (2018)
4. Y. Tomita, E. Hata, K. Momose, S. Takayama, X. Liua, K. Chikama, J. Klepp, C. Pruner, M. Fally, J. Mod. Opt. **63**(S3), S1–S31 (2016)
5. Y. Tomita, Holographic Nanoparticle-Photopolymer Composites, in *Encyclopedia of Nanoscience and Nanotechnology*, vol. 15, 2nd edn., ed. by H.S. Nalwa (American Scientific Publishers, Valencia, 2011), pp. 191–205
6. O.V. Sakhno, T.N. Smirnova, L.M. Goldenberg, J. Stumpe, Mater. Sci. Eng. C **28**, 28–35 (2008)
7. J. Burunkova, S. Kokenyesi, I. Csarnovics, A. Bonyár, M. Veres, A. Csik, Eur. Polym. J. **64**, 189–195 (2015)
8. D.I. Zhuk, J.A. Burunkova, I. Yu Denisyuk, G.P. Miroshnichenko, I. Csarnovics, D. Toth, A. Bonyar, M. Veres, S. Kokenyesi, Polymer **112**, 136–143 (2017)
9. D.J. Lockwood, Rayleigh and Mie Scattering, in *Encyclopedia of Color Science and Technology*, ed. by R. Luo (Springer, Berlin, 2015)
10. J.A. Burunkova, I.Y. Denisyuk, V. Bulgakova, S. Kokenyesi, $TiO_2$-acrylate. Solid State Phenom. **200**, 173–177 (2013)
11. J. Burunkova, I. Denisiuk, N. Vorzobova, S. Charnovych, S. Kokenyesi, Eur. Polym. J. **49**(10), 3072–3077 (2013)

12. K. Tanaka, K. Shimakawa (eds.), *Amorphous chalcogenide semiconductors and related materials* (Springer, New York, 2011)
13. A. Kikineshi, A. Mishak, Photoinduced Effects in Chalcogenide Glasses and their Application for Optical Recording, in *Physics and Applications of Non-Crystalline Semiconductors in Optoelectronics, NATO ASI Series*, vol. 3, ed. by A. Andriesh, M. Bertolotti (Kluwer Acad. Publ, Dordrecht, 1997), pp. 249–257
14. Y. Zha, M. Waldmann, C.B. Arnold, Opt. Mater. Express **3**(9), 1259–1272 (2013)
15. T.A. Guiton, C.G. Pantano, Chem. Mater. **1**(5), 558–563 (1989)
16. C. Tsay, E. Mujagić, C.K. Madsen, C.F. Gmachl, C.B. Arnold, Opt. Express **18**(15), 15523–15530 (2010)
17. I. Dehant, R. Danc, V. Kimmer, R. Shmol'ke, Infrakrajnaja spektroskopija polimerov, Moscow (1976)
18. Yu. Yu. Kercha, V. N. Vatulev, Infrakrasnye spektry i struktura poliuretanov, Kiev (1987)
19. L. Bellami, Infrakrasnye spektry slozhnyh molekul, Moscow (1963)
20. B.N. Tarasevich, *IK spektry osnovnyh klassov organicheskih soedinenij* (Spravochnye materialy, Moscow, 2012)
21. Y. Rabek, *Jeksperimenl'nye metody v himii polimerov*, vol. 1 (Mir, Moscow, 1983), p. 386
22. K. Kaminski, R. Wrzalik, M. Paluch, J. Zioło, C.M. Roland, J. Phys. Condens. Mater. **20**, 244121 (2008)
23. J.C. Maxwell Garnett, Philos. Trans. R. Soc. Lond. **203**, 385 (1904)
24. O. Wiener, Phys. Z. **5**, 332 (1904)
25. O. Wiener, Abh. Leipz. Akad. **32**, 509 (1912)
26. D.A.G. Bruggeman, Ann. Phys. **24**, 636 (1935)
27. K. Lichtenecker, Physik Z. **27**, 115–255 (1926)
28. N.A. Carlie, A solution-based approach to the fabrication of novel chalcogenide glass materials and structures, Clemson University, Thesis, p. 141, March 29, 2010
29. L.A. Golovan, VYu. Timoshenko, P.K. Kashkarov, UFN (Uspekhi Fizicheskikh Nauk) **177**(6), 619–638 (2007)
30. A.A. Al-Ghamdi, Vacuum **80**, 400–405 (2006)
31. J.C. Adam, X. Zhang, *Chalcogenide Glasses: Preparation, Properties and Applications. Woodhead Publishing series in electronic and optical materials* (Woodhead Publishing, Oxford, 2014)